

## Article

# Sludge Gasification Using Iron Bearing Metallurgical Slag as Heat Carrier: Characteristics and Kinetics

Zongliang Zuo <sup>1,2,\*</sup>, Tian Jing <sup>3</sup>, Jinmeng Wang <sup>2,4,†</sup>, Xinjiang Dong <sup>2</sup>, Yishan Chen <sup>2</sup>, Siyi Luo <sup>2,\*</sup> and Weiwei Zhang <sup>2</sup>

<sup>1</sup> State Key Laboratory of Complex Nonferrous Metal Resources Clean Utilization, Kunming University of Science and Technology, No. 727, Jingming South Road, Chenggong District, Kunming 650093, China

<sup>2</sup> School of Environmental and Municipal Engineering, Qingdao University of Technology, No. 777, Jialingjiang East Rd., Qingdao 266520, China

<sup>3</sup> Yingda Taihe Life Insurance Co., Ltd., Dongcheng District, Beijing 100005, China

<sup>4</sup> Thermal Science and Engineering Research Center, Shandong University, No. 27, Shanda South Rd., Jinan 250100, China

\* Correspondence: zuozongliangneu@163.com (Z.Z.); luosiyi666@126.com (S.L.)

† These authors contributed equally to this work.

**Abstract:** Waste heat recovery is a key problem to be solved for metallurgical slag. Furthermore, the heat source is a current bottleneck for sewage sludge gasification technology. At present, there is no complete process system for the thermochemical conversion of sludge driven by metallurgical slag waste heat. To recover the waste heat of slag, a granulation and waste heat recovery system using the sewage sludge gasification reaction is proposed in this paper. The sludge gasification kinetics were analyzed using thermogravimetry (TG). The active catalytic components in both Cu and Ni slag were determined using X-ray diffractometry (XRD) and X-ray photoelectron spectroscopy (XPS). The results show that the metallurgical slag could improve the decomposition rate of the sludge gasification reaction. The main catalytic components were Fe<sub>3</sub>O<sub>4</sub> and CaO for Cu slag and Ni slag, respectively. The conversion ratio was increased by 7.8% and 11.8%, while the activation energy decreased from 21.09 kJ/mol to 17.36 kJ/mol and 17.30 kJ/mol, respectively, when Cu slag and Ni slag were added. After oxidative modification, the catalytic function was enhanced for Cu slag, whereas it was weakened for Ni slag.

**Keywords:** sewage sludge; Cu slag; Ni slag; waste heat recovery; gasification

**Citation:** Zuo, Z.; Jing, T.; Wang, J.; Dong, X.; Chen, Y.; Luo, S.; Zhang, W. Sludge Gasification Using Iron Bearing Metallurgical Slag as Heat Carrier: Characteristics and Kinetics. *Energies* **2022**, *15*, 9223. <https://doi.org/10.3390/en15239223>

Academic Editor: Eliseu Monteiro

Received: 9 October 2022

Accepted: 1 December 2022

Published: 5 December 2022

**Publisher's Note:** MDPI stays neutral with regard to jurisdictional claims in published maps and institutional affiliations.



**Copyright:** © 2022 by the authors. Licensee MDPI, Basel, Switzerland. This article is an open access article distributed under the terms and conditions of the Creative Commons Attribution (CC BY) license (<https://creativecommons.org/licenses/by/4.0/>).

## 1. Introduction

Sewage sludge is a semi-solid material derived from urban and industrial sewage treatment. Sludge is a large amount of solid waste with huge output. The first mock exam of sewage sludge treatment was focused on dewatering and landfill [1]; however, through this method, the toxic and harmful substances in sludge caused serious environmental problems. Therefore, recycling treatment methods with reduced environmental impact are needed urgently.

Pyrolysis or gasification technology, as a thermal conversion technology for the energy utilization of solid raw materials, has become an important direction for carbonaceous organic solid disposition [2,3]. Gasification technology is a process of cracking organic units, removing volatile components, and forming solid coke slag under high-temperature reaction conditions with a gasification agent [4]. The gasification process usually coexists with the pyrolysis process [5]. The steam and carbon dioxide produced during the pyrolysis process can be used as gasification agents to participate in the gasification reaction [6]. Pyrolysis gas produced by pyrolysis or gasification is rich in gaseous hydrocarbons, hydrogen, and carbon monoxide [7,8].

Sludge is rich in organic matter and combustible components, which is a sufficient condition for gasification as a raw material [9,10]. Using gasification technology to extract carbon from sludge can convert organic matter into clean and cheap energy while avoiding secondary pollution [11,12]. However, sludge has high ash, high moisture, and low volatile organic compounds. Sludge treatment requires a lot of heat [13]. It requires at least 360 MJ of energy per ton of sludge to be treated with 80% water. It is of great significance to find a stable and economical heat source [14,15].

Furthermore, Cu and Ni slag are typical by-products discharged from the smelting process, whereby about 2.2 tons of slag can be produced for every ton of Cu or Ni [16]. At present, these slags are typically treated by water quenching in smelting enterprises [17]. This treatment method not only fails to recover high-temperature waste heat but also wastes water resources and produces substantial pollution [18]. Slag waste heat recovery and resource utilization are hot issues in the metallurgical industry [6,12,19]. The treatment temperature of slag is about 1300 °C, and the equivalent of about 48 kg of standard coal is needed to provide the heat required for the pyrolysis of one ton of sludge. In addition, Cu slag and Ni slag contain valuable metals such as Fe and Ca; the mass fraction of Fe can reach more than 40%, which can be used as a catalyst and carbon pore structure modifier in the sludge pyrolysis process [20]. Moreover, the gasification reaction can consume oxidation agents (such as CO<sub>2</sub>) and produce high value-added gas [21,22]. At present, the catalysts used in sludge gasification or pyrolysis mainly include alkali metal [23], carbon-based catalysts [24], transition metal, and natural ores (such as iron ore [25] and quartz sand [26]). The oxidation agents commonly used for sludge gasification include air, steam, oxygen, CO<sub>2</sub>, or a mixture [27].

High-value material cannot be used to process low-value material. Therefore, the key is to treat waste with waste. Moreover, metallurgical slag itself contains alkali metals, representing potential catalytically active components [28,29]. Alkali metal catalysts have a certain ability to decompose tar. However, the composition of metallurgical slag is complex. When it is used as a heat carrier, its catalytic characteristics and active components are difficult to determine. Basic research on the catalysis of blast furnace slag was carried out by Sun [30]; however, the metal content of blast furnace slag is relatively low. In non-ferrous metallurgical industries, the metal content in slag (such as Cu slag or Ni slag) is higher than that in blast furnace slag.

Considering the waste heat recovery demand of non-ferrous metallurgical slag and the treatment demand of sewage sludge, a technical system is proposed as shown in Figure 1. The metallurgical slag granulation and waste heat recovery technology system is shown in Figure 1. It contains a granulator and gasification reactor. Firstly, molten slag is granulated into solid slag particles with a diameter <5 mm at 1100 °C. Then, slag particles enter the gasification reactor. In a gasification reactor, hydrous municipal sludge (the moisture content is about 70%) and CO<sub>2</sub> flow into the reactor. The organic matters (carbon and hydrogen contained in sludge) and fixed carbon react with carbon dioxide. These endothermic gasification reactions take place at this stage. As products, after condensation, a mixture of gas of CO<sub>2</sub>, CO, H<sub>2</sub>, and H<sub>2</sub>O is produced. During this process, slag particles are cooled to 100 °C. The syngas can be used as combustion fuel to provide heat in the smelting process of copper or nickel. With this technology system, slag particles are cooled and can be used as cement additives for resource utilization. Mass and energy analysis of the waste heat cascade recovery of copper slag have been analyzed in the author's previous study [6]. Compared with multi-stage waste heat recovery [6], the device and process of the system in this research are simple. Moreover, the system uses smoke as a gasification agent, which has lower carbon emissions and is a carbon neutralization technology path. By calculation and analysis, 21.0 kg of sludge and 8.48 kg of carbon dioxide are consumed when 1 ton of metallurgical slag is disposed of using the metallurgical slag granulation and waste heat recovery technology system.

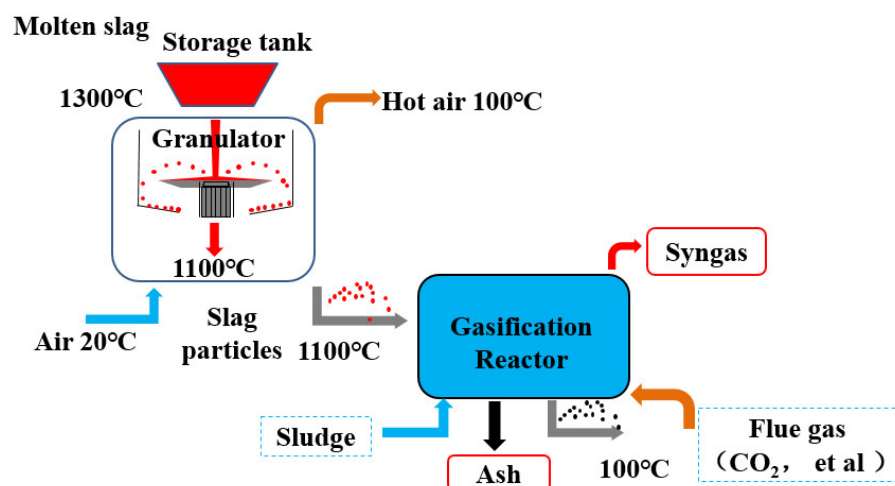


**Figure 1.** Metallurgical slag granulation and waste heat recovery technology system.

The characteristics of the sludge gasification reaction with CO<sub>2</sub> as an oxidation agent were studied using two kinds of typical raw metallurgical slags as the heat carrier. Mass loss via gasification was analyzed using thermogravimetry (TG). The active components in both Cu slag and Ni slag were determined through phase detection and composition determination using X-ray diffractometry (XRD) and X-ray photoelectron spectroscopy (XPS). Furthermore, the activation energy and kinetic parameters were calculated when the heat carrier was added.

## 2. Material and Methods

### 2.1. Material

In this experiment, Cu slag and Ni slag sample were obtained from a flash-smelting metallurgical plant in China. Sludge is collected from a sewage treatment plant in Qingdao, China. The slag and sludge were pulverized (100 mesh) using a mechanical crusher. Then, samples were fully dried in a constant temperature blast drying oven at 105 °C for 4 h. The chemical composition of Cu slag and Ni slag are shown in Tables 1 and 2, respectively. As indicated, SiO<sub>2</sub>, FeO, Fe, CaO, and Al<sub>2</sub>O<sub>3</sub> were the main components. As there is no dilution treatment for Cu slag, the content of Cu was 0.68%, which meets the standard of copper ore. The composition of Ni slag differed in that CaO SiO<sub>2</sub>, MgO, FeO, and Fe were the main components. The evaluation was conducted using a proximate analyzer (SDTGA5000). The phases in raw materials were identified by XRD using Cu-K $\alpha$  radiation operating at 30 kV and 40 mA, and diffraction data were recorded by continuous scanning with a step of 10°·min<sup>-1</sup>. Additionally, the XPS patterns of Cu slag and Ni slag were obtained using an XPS analyzer (spot size 400  $\mu$ m; source gun type, Al K $\alpha$ ; energy step size, 1.0 eV for survey results; the number of energy steps, 1361). The XPS test curve was fitted and analyzed using the XPSPEAK41 software, and the spectrum was corrected by setting the C1s binding energy to 284.6 eV.

**Table 1.** Chemical composition of Cu slag.

FeO	SiO <sub>2</sub>	TFe	CaO	Mfe	Al <sub>2</sub> O <sub>3</sub>	Zn	Na	MgO	Cu
24.63	31.77	27.19	9.58	7.70	6.24	4.85	3.02	2.53	0.68

**Table 2.** Chemical composition of Ni slag.

CaO	Tfe	SiO <sub>2</sub>	MgO	FeO	Mfe	Mn	TiO <sub>2</sub>	Cu	Ni
47.28	16.42	13.73	7.15	6.67	6.05	3.45	0.79	0.013	<0.01

Through drying experiments, it was found that the moisture content in municipal sludge was 74.9%. After drying, the industrial analysis results of municipal sludge are shown in Table 3, which highlights the volatile and fixed carbon of municipal sludge at 52.46% and 7.3% as the main gasification reactant, along with low organic content.

**Table 3.** Proximate analysis of municipal sludge, wt%.

Sample	Moisture	Volatile	Ash	Fixed Carbon
Municipal sludge	0.01	52.46	40.23	7.30

## 2.2. Methods

A thermodynamic analyzer was employed in this experiment. The slag sample and municipal sludge were first mixed and ground in a crucible. Then they were placed in a high-purity aluminum crucible and mixed sufficiently using an aluminum wire stirrer. The protective gas and reaction gas was N<sub>2</sub> and CO<sub>2</sub>, respectively. The flow rates were both 50 mL/min, as controlled by flow meters. The purity of N<sub>2</sub> used in this study was 99.9%. In each experiment, about 10 mg of the sample was heated from 100 °C to 800 °C~1000 °C at a heating rate of 10~20 °C/min. The mass loss ratio of the sample was detected and recorded. The effects of different heating rates, reaction temperatures, and types of heat carriers on the reaction rate and weight loss rate were investigated. An equal mass of SiO<sub>2</sub> was added as the blank experimental control in the crucible to correct for the baseline of the reaction. The experimental method was the same as described in our previous research work [19].

## 3. Results and Discussions

### 3.1. Characteristics of Slag Heat Carrier

As a heat carrier, slag provides energy for the chemical reaction; thus, its phase composition and surface properties were determined by chemical reaction. Figures 2 and 3 present the XRD patterns of the waste slags before the reduction reaction. As shown in Figure 2, fayalite was the main component of the slag. However, the composition of copper slag was complex, and several crystal forms exist. There were many miscellaneous phases in Cu slag, such as magnetite (Fe<sub>3</sub>O<sub>4</sub>), wüstite (FeO), silicon oxide (SiO<sub>2</sub>), and cuprite (Cu<sub>2</sub>O). As shown in Figure 3, the main phases detected in the XRD patterns of Ni slag were lamite (Ca<sub>2</sub>SiO<sub>4</sub>) and calcium silicate (Ca<sub>3</sub>SiO<sub>5</sub>). Due to the existence of Ca, Mg, and Al, the compound phase of slag was complex, such as Ca<sub>54</sub>MgAl<sub>2</sub>Si<sub>16</sub>O<sub>90</sub>.

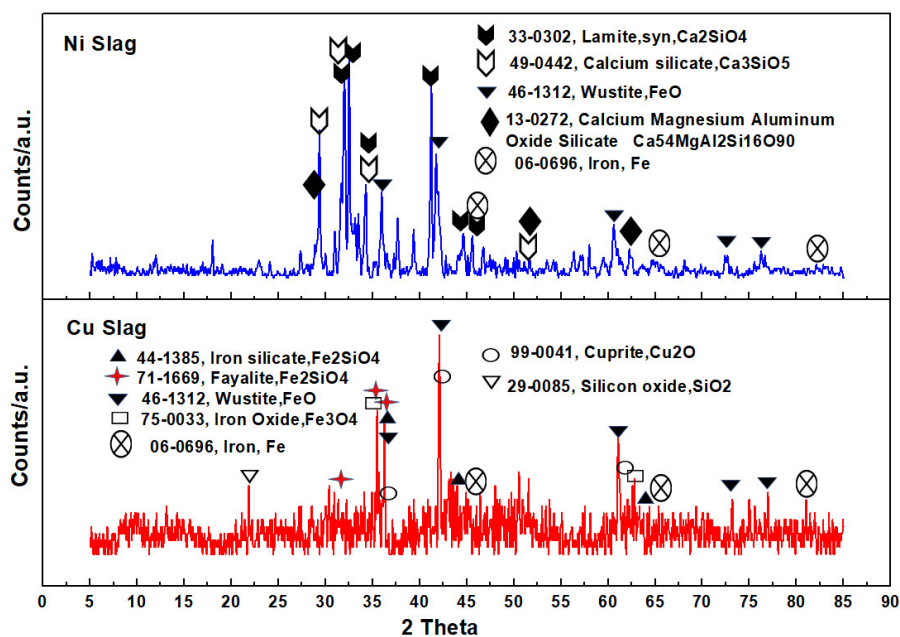


Figure 2. XRD patterns of Cu slag and Ni slag.

To determine the surface atomic type and concentration of Cu slag and Ni slag, XPS analysis was carried out as shown in Figure 3. Based on the results of peak splitting XPS results, the basic information of atoms with different orbitals was obtained as shown in Table 4. We could also determine semi-quantitatively from the peak areas that the Fe, Si, and Cu contents were higher in Cu slag than in Ni slag. Furthermore, the Ca content in Ni slag was much higher than that in Cu slag. This is consistent with the results of elemental analysis. We found that the  $\text{SiO}_2$  in Cu slag was mainly present in the form of  $2\text{FeO}\cdot\text{SiO}_2$ . The Ca in Ni slag was mainly present in the form of  $\text{CaO}$ . Both of them are potentially catalytic components.

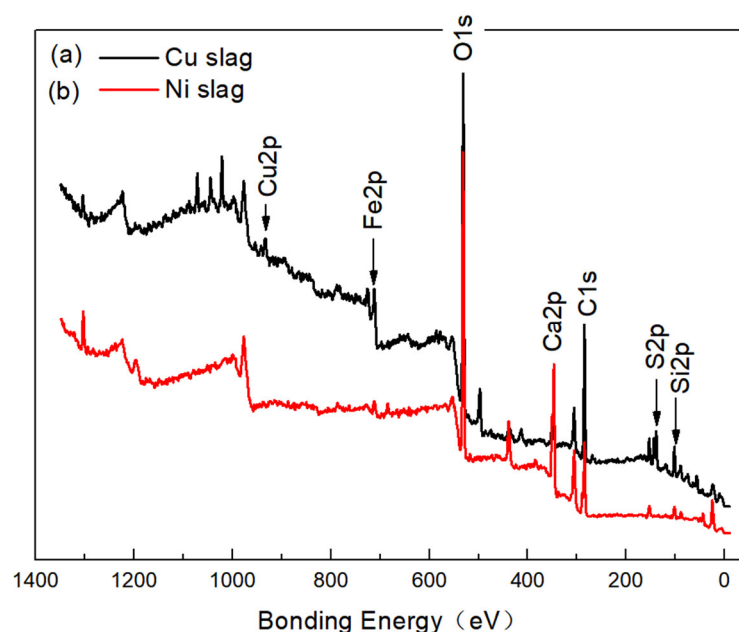


Figure 3. Survey scan XPS spectra of Cu slag and Ni slag.

**Table 4.** Peak table of Cu slag and Ni slag.

Sample	Name	Start BE	Peak BE	End BE	Height CPS	FWHM (eV)	Area (P) CPS. eV
Cu slag	Si2p	109.76	102.06	94.86	3261.75	1.75	6695.26
	S2p	174.76	162.82	156.86	387.82	3.04	2406.07
	C1s	297.76	284.8	278.86	16,680.03	1.26	27,618.2
	Ca2p	359.76	347.35	339.86	3143.93	1.62	11,346.11
	O1s	544.76	531.06	524.86	33,295.91	2.32	85,416.3
	Fe2p	739.71	711.09	699.91	4352.76	4.19	40,033.9
	Ni2p	887.71	862.3	843.91	409.43	0.12	7407.4
	Cu2p	966.71	932.34	924.91	3363.35	2.1	22,266.04
	Ni slag	Si2p	109.41	102.03	94.51	896.45	2.46
S2p		174.41	169.1	156.51	178.68	0.15	668.68
C1s		297.41	284.8	278.51	7267.74	1.54	16,835.57
Ca2p		359.41	347.03	339.51	12177.8	1.84	38,357.95
O1s		544.41	531.27	524.51	25,476.15	2.35	68,628.93
Fe2p		739.36	710.81	699.56	1014	4.29	11,257.13
Ni2p		883.36	863.02	843.56	330.64	0.31	5168.47
Cu2p		966.36	940.41	924.56	404.94	0.52	5524.79

### 3.2. Sludge Gasification Characteristics Based Slag as Heat Carrier

Firstly, blank control group experiments were conducted. Figures 4 and 5 show the TG and DTG curves of sludge gasification and pyrolysis reactions. The pyrolysis reaction of sludge occurred in the N<sub>2</sub> atmosphere while the gasification reaction of sludge occurred in the CO<sub>2</sub> atmosphere. According to the decomposition degree of sludge, the gasification reaction was more thorough than the pyrolysis reaction. The main factor involved in the pyrolysis reaction is the precipitation of volatile substances in sludge. In contrast, the gasification reaction also includes the reaction of carbonaceous substances with the gasification agent, i.e., oxygen. For example, carbon substances in sludge can react with CO<sub>2</sub> to produce CO. Following the pyrolysis reaction, the ash and fixed carbon in the sludge were retained, accounting for 72.11% of the sample mass. Following the gasification reaction, they accounted for 58.85% of the sample mass. The quality difference was greater than the content of fixed carbon in the industrial analysis as shown in Table 3. This is because the gasification of CO<sub>2</sub> involves some refractory macromolecular organics that escape from the reactor. Furthermore, through the DTG curve, we can see that the temperature corresponding to the maximum weight loss rate of sludge pyrolysis and gasification was almost the same. Moreover, it can be seen from Figures 4 and 5 that the weight loss range of sludge gasification in carbon dioxide atmosphere is mainly in 200–600 °C, and two peaks of weight loss appear at 200–400 °C and 400–600 °C, respectively. The temperature range of the peak is consistent with the TGA profile obtained by Zhao et al. [31] in air atmosphere. The termination temperatures of pyrolysis and gasification reactions were different; about 800 °C and 700 °C, respectively. Luo et al. [32] found that the gas production of sludge and metallurgical slag continued to increase above 800 °C. The reason for this difference is that the fixed carbon content in the sludge used in this paper is lower than that in the reference, and the gasification agent used is different.

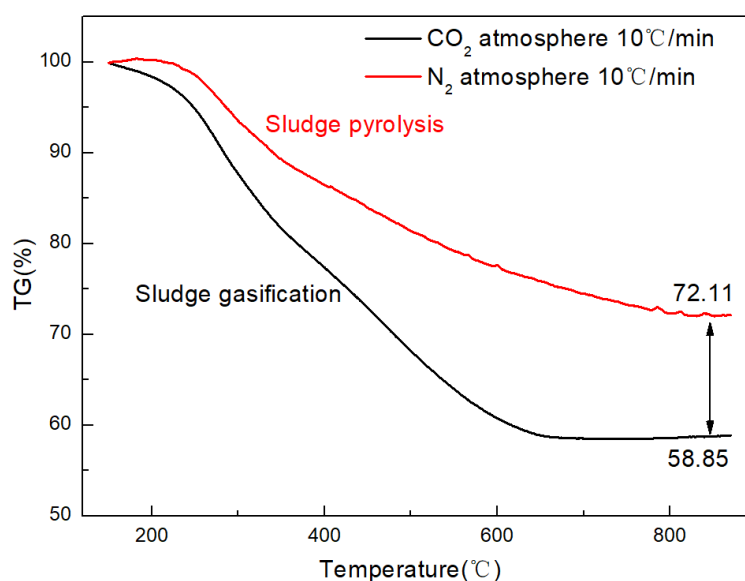


**Figure 4.** TG curves of sludge gasification and pyrolysis reactions.

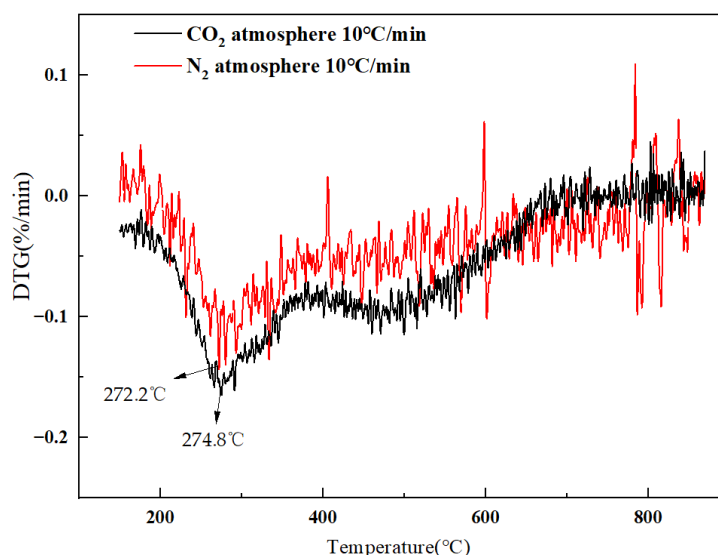


**Figure 5.** DTG curves of sludge gasification and pyrolysis reactions.

The TG and DTG curves of sludge gasification with different heating rates are shown in Figures 6 and 7. To reflect the real situation of catalysis, we introduced a mixture of equal-quality sludge and silica as a blank control. We can see that the addition of metallurgical slag improved the decomposition rate of the sludge gasification reaction. This confirms the catalytic effect of metallurgical slag on the sludge gasification reaction. Without the slag heat carrier, the terminal mass of the sample is 79.32%. When Cu slag was added at the same heating rate, the terminal mass of the sludge sample decreased to 77.70%. In contrast, when Ni slag was added at the same heating rate, the terminal mass of the sludge sample decreased to 76.88%. The conversion ratio was increased by 7.8% and 11.8% when using Cu slag and Ni slag as the heat carriers, respectively. Through the comparison of different heating rates, it can be found that the conversion ratio at 10 °C/min was higher than that at 20 °C/min, which was mainly because sufficient time was left for the gasification reaction at a lower heating rate. Catalysis caused a change in conversion but the reaction rate changed little, as shown in Figure 7. At 10 °C/min and 700–800 °C, the catalytic action of Cu slag caused a secondary reaction.

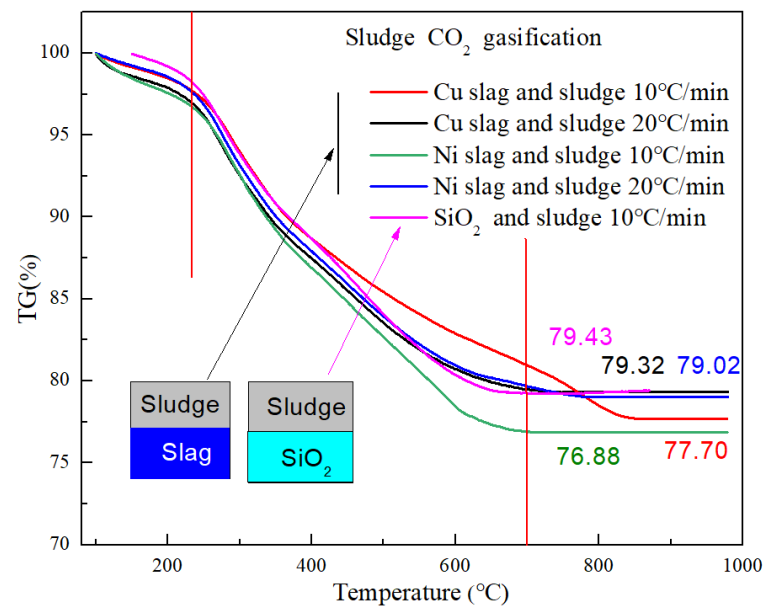


Figure 6. TG curves of sludge gasification with different heating rates.

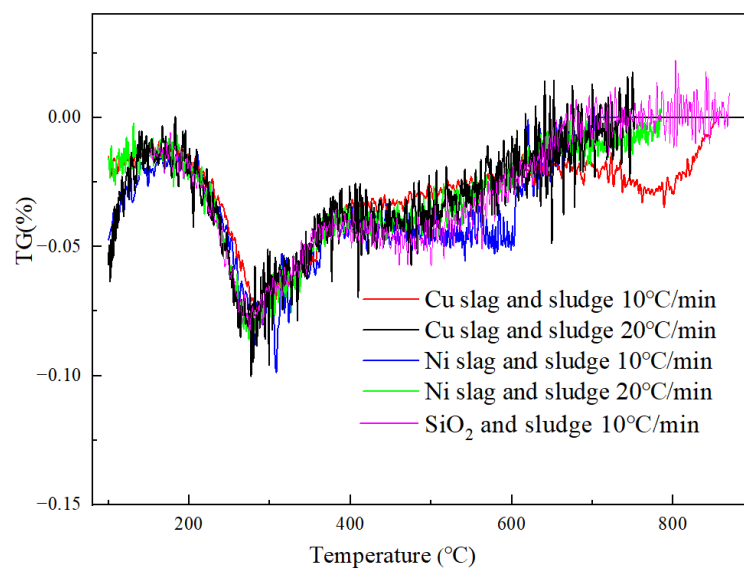
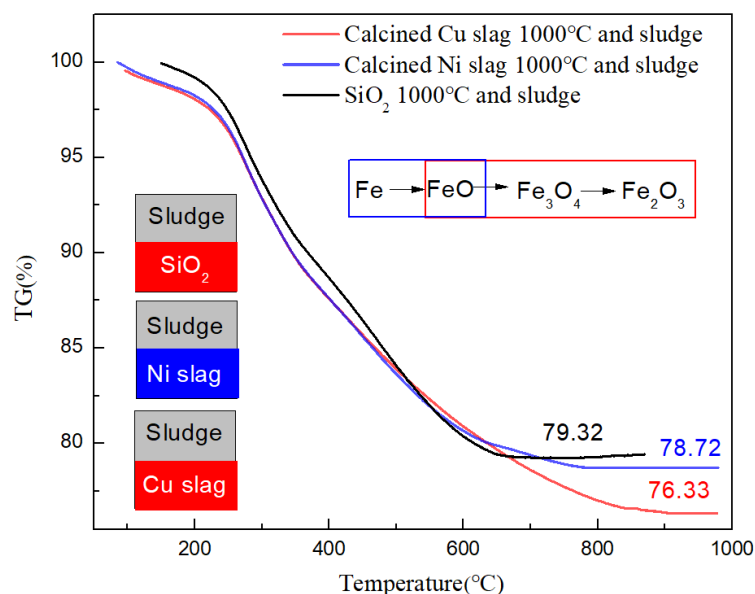
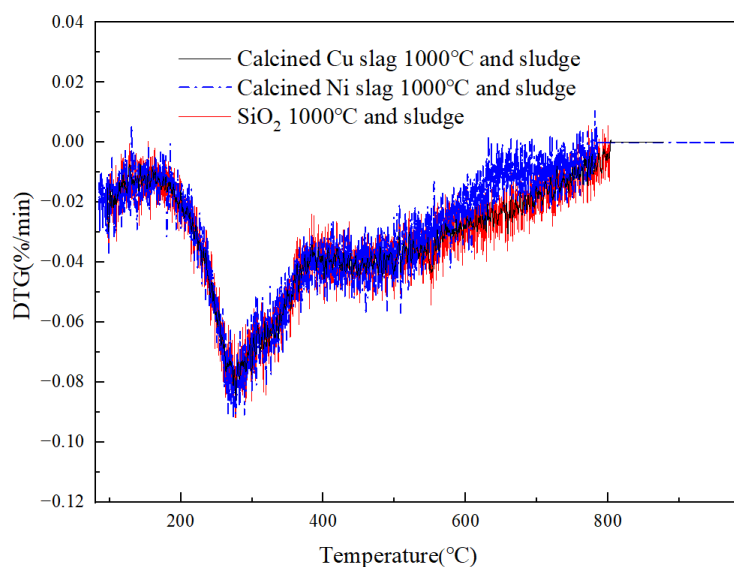


Figure 7. DTG curves of sludge gasification with different heating rates.

Cu slag is rich in metals, such as iron. Thus, modifying the metal in slags via calcination can improve the content of iron oxide and its catalytic performance. From the perspective of engineering application, the effective oxidation of metals can be realized by blowing enough air into the granulator. Cu slag and Ni slag were calcined fully at 1000 °C in a furnace for 1 h and then taken out. The sludge gasification reaction experiment was carried out. TG and DTG curves of sludge gasification with calcined slags are shown in Figures 8 and 9. In the comparison between Figures 6 and 8, it can be seen that the catalytic capacity of oxidized Cu slag is improved. The quality of terminated materials was further reduced from 77.70% to 76.33%. The catalytic effect of copper slag after oxidation is more obvious, which is consistent with the finding of Deng et al. [33]. The conversion ratio was increased by 14.5% and 2.9% when using calcined Cu slag and Ni slag as heat carriers, respectively, compared with sludge gasification using SiO<sub>2</sub> as the heat carrier.



**Figure 8.** TG curves of sludge gasification with calcined slags.



**Figure 9.** DTG curves of sludge gasification with calcined slags.

The comparison results of the catalytic function of different heat carriers are shown in Figure 10. XRD patterns of calcined Cu slag and Ni slag are shown in Figure 11. According to the change in metal valence on the surface of the heat carrier, its catalytic effect on sludge differed.

After calcination and oxidation, the oxidation reaction of iron and copper occurred and the phase peaks of  $\text{Fe}_2\text{O}_3$  and  $\text{MgFe}_{2+3}\text{O}_4$  appeared in Cu slag. The catalytic effect on sludge gasification was enhanced by  $\text{Fe}_2\text{O}_3$  and  $\text{MgFe}_{2+3}\text{O}_4$ . It should be noted that  $\text{MgFe}_{2+3}\text{O}_4$  is a transition state of  $\text{Fe}_3\text{O}_4$  and  $\text{Fe}_2\text{O}_3$  forming a complex with  $\text{MgO}$ , as shown in Equation (1). Its essence is the transformation from  $\text{FeO}$  to  $\text{Fe}_3\text{O}_4$ , as shown in Equation (2). Thus, the termination reaction mass loss ratio was further improved from 22.3% to 23.67%. The phase conversion can be proved by the XRD patterns in Figures 2 and 11. The oxidation reaction in Cu slag is shown in Equations (1)–(4). Compared with  $\text{FeO}$  in the initial Cu slag, the structures of  $\text{Fe}_3\text{O}_4$  and  $\text{Fe}_2\text{O}_3$  in the calcined Cu slag are unstable, with high catalytic activity. The variation of Fe element in copper slag after oxidation calcination obtained from the above XRD patterns is consistent with the discovery of Zhao et al. [34].

After the calcination of Ni slag, oxidation of iron occurred, as shown in Equation (5). The phase peaks of FeO in Ni slag become stronger, as shown in Figure 10. Furthermore, another form of  $\text{MgFe}_{2+3}\text{O}_4$  appeared, albeit with low content. FeO can be easy to combine with  $\text{SiO}_2$  to form olivine, an extremely stable structure. As an alkaline metal oxide, CaO has good catalytic activity in its original state. However, after calcination and oxidation, the coating of FeO decreased the catalytic activity of CaO. The termination reaction mass loss ratio decreased from 23.12% to 21.28%. In other words, calcination oxidation was beneficial to Cu slag but unfavorable to Ni slag.

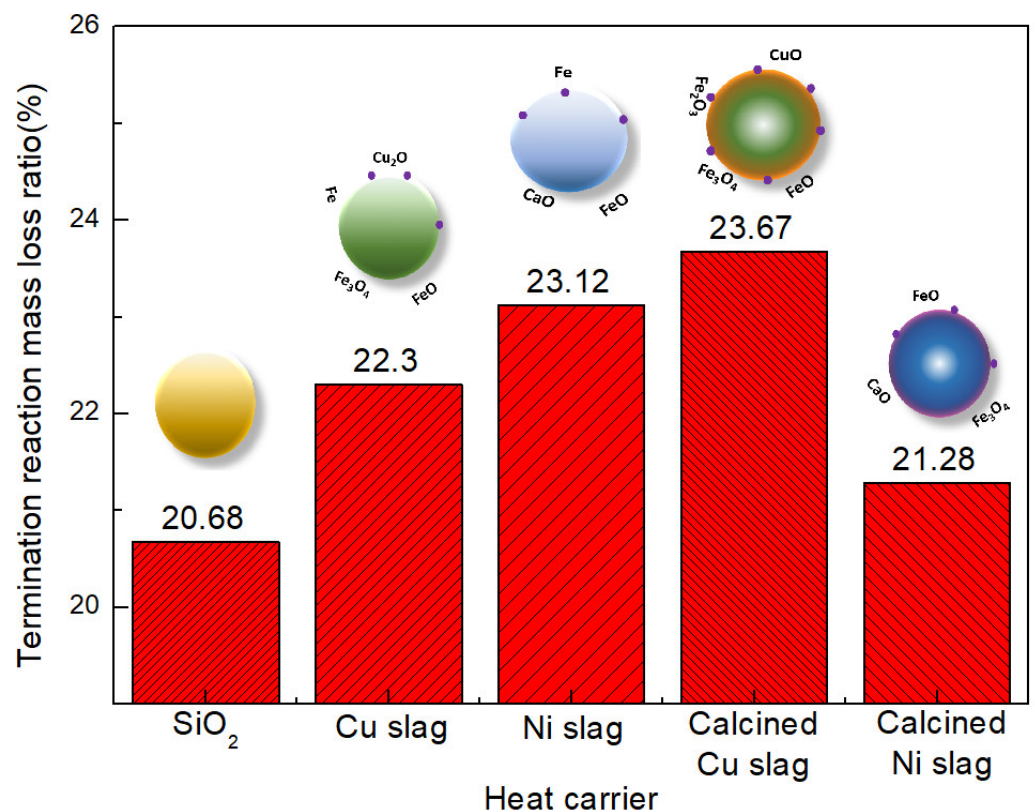
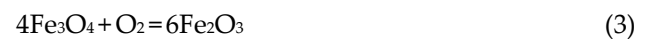
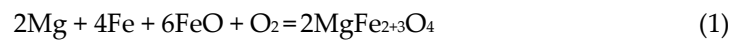


Figure 10. Termination reaction mass loss ratio with different heat carriers.

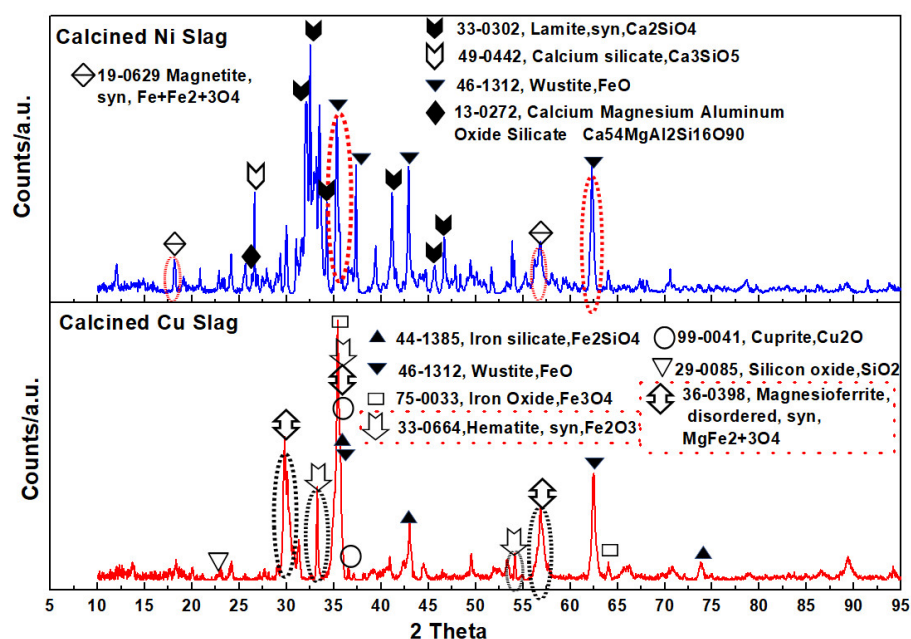


Figure 11. XRD patterns of calcined Cu slag and Ni slag.

### 3.3. Sludge Gasification Kinetics Using Slag as Heat Carrier

In this research, the Coats–Redfern method is selected to analyze the above dynamic parameters. According to the law of mass conservation, the mass loss rate in the process of sludge gasification reaction can be expressed as:

$$\frac{d\alpha}{dt} = k(1 - \alpha)^n \quad (6)$$

where  $n$  is the reaction order,  $\alpha$  is sludge gasification conversion rate (%), and  $k$  is Arrhenius constant. The expressions of  $\alpha$  and  $k$  are as follows:

$$\alpha = \frac{m_0 - m}{m_0 - m_e} \quad (7)$$

$$k = Ae^{\frac{-E}{RT}} \quad (8)$$

where  $m_0$  is the initial mass of the material (g),  $m$  is the mass of the material at a certain moment in the reaction process (g),  $m_e$  is the mass of the material when the reaction is terminated (g),  $A$  is pre-exponential factor,  $E$  is the activation energy (kJ/mol),  $R$  is the molar constant of gas (8.314 J/(mol·K)), and  $T$  is the thermodynamic temperature (K).

The heating rate is defined as follows:

$$\beta = \frac{dT}{dt} \quad (9)$$

Combined with the above formula, we can obtain:

$$\frac{d\alpha}{dt} = \frac{A}{\beta} e^{\frac{-E}{RT}} (1 - \alpha)^n \quad (10)$$

Both sides can be obtained by integrating and shifting terms.

$$\int_0^\alpha \frac{d\alpha}{(1-\alpha)^n} = \frac{A}{\beta} \int_{T_0}^T e^{-\frac{E}{RT}} dT \quad (11)$$

The logarithms on both sides of Equation (11) can be taken. When  $n = 1$ , the equation can be transformed as follows:

$$\ln\left[-\frac{\ln(1-\alpha)}{T^2}\right] = \ln\left[\frac{AR}{E\beta}\left(1-2\frac{RT}{E}\right)\right] - \frac{E}{RT}. \quad (12)$$

When  $n \neq 1$ :

$$\ln\left[\frac{1-\ln(1-\alpha)^{1-n}}{T^2(1-n)}\right] = \ln\left[\frac{AR}{E\beta}\left(1-2\frac{RT}{E}\right)\right] - \frac{E}{RT}. \quad (13)$$

$\frac{E}{RT} \gg 1$ , thus,  $a = -E/R$ ,  $X = 1/T$ , and  $b$  is as follows:

$$b = \ln\left[\frac{AR}{E\beta}\left(1-2\frac{RT}{E}\right)\right] \approx \ln\left(\frac{AR}{E\beta}\right). \quad (14)$$

When  $n = 1$ ,  $Y$  is as follows:

$$Y = \ln\left[-\frac{\ln(1-\alpha)}{T^2}\right]. \quad (15)$$

When  $n \neq 1$ ,  $Y$  is as follows:

$$Y = \ln\left[\frac{1-\ln(1-\alpha)^{1-n}}{T^2(1-n)}\right]. \quad (16)$$

Thus, the function ' $Y = aX + b$ ' can be obtained. Through the thermogravimetric curve obtained from the sludge gasification experiment, combined with the fitting Equations (15) and (16), the relationship between the activation energy  $E$  and the pre-exponential factor  $a$  could be obtained. During the fitting calculation, the reaction orders were calculated, respectively, when the reaction orders were 0.5, 1, 1.5, and 2 so as to compare and determine the actual reaction orders. Lastly, the kinetic fitting curves of the sludge gasification reaction under different experimental conditions were drawn. The appropriate reaction order was selected according to the correlation coefficient  $R^2$  of the curve.

The kinetic parameter values of the sludge gasification reaction under experimental conditions can be derived from the data in Table 5. Heat carrier  $\text{SiO}_2$  had little effect on the reaction. This is mainly due to the stable nature of silica. In the actual system process, the existence of a heat carrier may improve the heat and mass transfer rate, but this is not reflected by the dynamics. When the heating rate was  $10^\circ\text{C}/\text{min}$ , with Cu and Ni slag as the heat carriers, the activation energy decreased from 21.09 kJ/mol to 17.36 kJ/mol and 17.30 kJ/mol, respectively. According to the calculation results of activation energy, we can see that both Cu slag and Ni slag could reduce the activation energy of the gasification reaction, while the catalytic potential of alkali metals in the nickel slag was stronger. Therefore, the activation energy of the gasification reaction catalyzed by the Cu slag heat carrier was lower than that catalyzed by the Ni slag heat carrier. The results also show that the catalytic effect of CaO in Ni slag was stronger than iron oxides in Cu slag.

Furthermore, after oxidation, a reversal of the activation energy of Ni slag and Cu slag occurred. The activation energy of Cu slag decreased to 14.53 kJ/mol, indicating that the catalytic activity of copper slag is strengthened after oxidation. In contrast, the activation energy of Ni slag increased from 17.30 to 17.86 kJ/mol. This further proves that the catalytic effect of oxidation treatment on Cu slag was strengthened, while that on Ni slag

was inhibited, as shown in Figure 11. This was mainly due to the change in catalytic active components.

**Table 5.** Kinetic parameters of municipal sludge gasification in experiment conditions.

No	Heat Carrier	Heating Rate (°C/min)	Atmosphere	Temperature Region of Maximum Mass loss (°C)		R <sup>2</sup>	Activation Energy (kJ/mol)	Reaction Coefficient
1	-	10	N <sub>2</sub>	247	352	0.998	21.18	2
2	-	10	CO <sub>2</sub>	237	347	0.998	21.93	2
3	SiO <sub>2</sub>	10	CO <sub>2</sub>	227	302	0.995	21.09	0.5
4	Cu slag	20	CO <sub>2</sub>	237	352	0.984	17.93	1
5	Cu slag	10	CO <sub>2</sub>	262	367	0.993	17.36	2
6	Ni slag	20	CO <sub>2</sub>	247	347	0.995	18.10	1.5
7	Ni slag	10	CO <sub>2</sub>	252	352	0.996	17.30	2
8	Calcined-Cu slag	10	CO <sub>2</sub>	247	372	0.998	14.53	2
9	Calcined-Ni slag	10	CO <sub>2</sub>	262	372	0.993	17.86	2

From the perspective of the catalytically enhanced gasification reaction in the technical system, the treatment methods of Ni slag and Cu slag were different. As shown in Figure 12, Cu slag is metallurgical slag rich in divalent iron with a phase of 2FeO·SiO<sub>2</sub>. This kind of slag should be oxidized in the granulation process to transform the internal iron-containing components into magnetite and hematite minerals. Air can be selected as the coolant in the granulation process. Ni slag is a metallurgical slag with low iron content, which exists in the form of metal. This kind of slag should not be oxidized in the granulation process. Flue gas can be selected as the coolant in the granulation process.

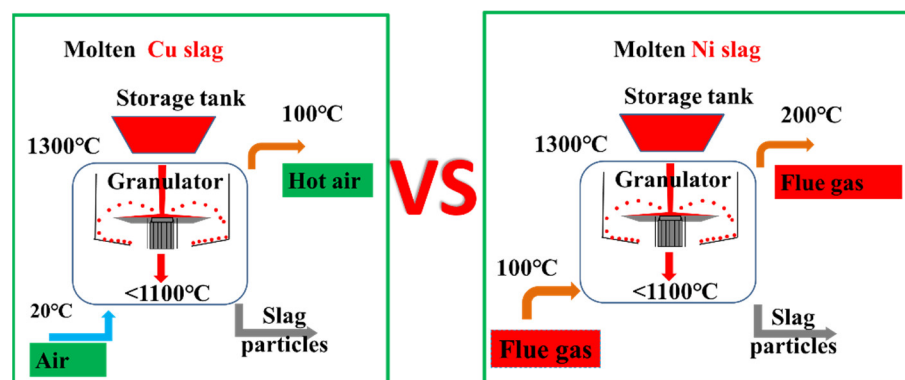


**Figure 12.** Comparison of treatment technology Cu slag and Ni slag.

#### 4. Conclusions

A metallurgical slag granulation and waste heat recovery technology system for iron-bearing metallurgical slag was proposed in this research. The system uses smoke as a gasification agent, which provides a path to carbon neutralization technology. The kinetics of the sludge gasification reaction with CO<sub>2</sub> were studied, using two kinds of typical raw metallurgical slags as the heat carriers and catalysts.

- (1) There were many miscellaneous phases in Cu slag, such as magnetite (Fe<sub>3</sub>O<sub>4</sub>), wüstite (FeO), silicon oxide (SiO<sub>2</sub>), and cuprite (Cu<sub>2</sub>O). The main phases of Ni slag were lamite (Ca<sub>2</sub>SiO<sub>4</sub>) and calcium silicate (Ca<sub>3</sub>SiO<sub>5</sub>). The Fe, Si, and Cu content in Cu slag

was higher compared to Ni slag. The Ca content in Ni slag was much higher compared to Cu slag.

- (2) Metallurgical slag could improve the decomposition rate of the sludge gasification reaction. The conversion ratio was increased by 7.8% and 11.8% when using Cu slag and Ni slag as the heat carriers, respectively. The main catalytic component were  $\text{Fe}_3\text{O}_4$  and  $\text{CaO}$ . The catalytic function of alkali metals in Ni slag was stronger than that of  $\text{Fe}_3\text{O}_4$  in Cu slag. Correspondingly, the activation energy of the gasification reaction catalyzed by Cu slag was lower than that catalyzed by Ni slag. Using Cu and Ni slag, activation energy decreased from 21.09 kJ/mol to 17.36 kJ/mol and 17.30 kJ/mol, respectively.
- (3) After modification, the active components changed.  $\text{Fe}_2\text{O}_3$  and  $\text{MgFe}_{2+3}\text{O}_4$  were the active components in the modified Cu slag and the catalytic function was enhanced. After modification,  $\text{CaO}$  remained the active component in Ni slag, but it was weakened by the generation of  $\text{FeO}$ . In Ni slag,  $\text{FeO}$  was combined with  $\text{SiO}_2$  to form olivine, which is an extremely stable structure. The conversion ratio increased by 14.5% and 2.9% when using calcined Cu slag and Ni slag, respectively, compared with sludge gasification using  $\text{SiO}_2$ .
- (4) Oxidation modification is beneficial to the catalytic function of Cu slag but unfavorable to that of Ni slag. Thus, different treatment methods should be applied to Cu slag and Ni slag. Cu slag should be oxidized in the granulation process to transform the internal iron-containing components into magnetite and hematite minerals. On the other hand, Ni slag should not be oxidized in the granulation process.

**Author Contributions:** Z.Z., T.J., J.W. and X.D. conceived and planned the experiments. Z.Z., S.L., X.D. and Y.C. carried out the experiments. T.J., J.W. and S.L. contributed to sample preparation. Z.Z., T.J., J.W., X.D., Y.C., S.L. and Weiwei Zhang contributed to the interpretation of the results. Z.Z. took the lead in writing the manuscript. All authors provided critical feedback and helped shape the research, analysis and manuscript. All authors have read and agreed to the published version of the manuscript.

**Funding:** This research has been supported by the Natural Science Foundation of China (52104397), the Natural Science Foundation of Shandong Province (ZR2020QE150), Open Project of State Key Laboratory of Complex Nonferrous Metal Resources Clean Utilization (CNMRCUKF2207), Science and Technology Project of Qingdao West Coast New Area (2020-35).

**Conflicts of Interest:** The authors declare that they have no known competing financial interests or personal relationships that could have appeared to influence the work reported in this paper.

## References

1. Fonts, I.; Gea, G.; Azuara, M.; Ábrego, J.; Arauzo, J. Sewage sludge pyrolysis for liquid production: A review. *Renew. Sustain. Energy Rev.* **2012**, *16*, 2781–2805.
2. Shibata, S. *Inventorprocede de Fabrication d'une Huille Combustible a Partir de Boue Digeree*; France, 1939.
3. Taro, S.; Nakorn, W. Kinetic Analyses of Biomass Pyrolysis Using the distributed Activation Energy Model. *Fuel* **2008**, *87*, 414–421.
4. Liu, J.; Huang, Z.; Chen, Z.; Sun, J.; Gao, Y.; Wu, E. Resource utilization of swine sludge to prepare modified biochar adsorbent for the efficient removal of Pb(II) from water. *J. Clean. Prod.* **2020**, *257*, 120322.
5. Javier, Á.; Jesus, A.; Lius, S.J.; Alberto, G.; Tomas, C.; Mirasol, J.R. Structural changes of sewage sludge char during fixed-bed pyrolysis. *Ind. Eng. Chem. Res.* **2009**, *48*, 3211–3221.
6. Zuo, Z.; Feng, Y.; Li, X.; Luo, S.; Ma, J.; Sun, H.; Bi, X.; Yu, Q.; Zhou, E.; Zhang, J.; et al. Thermal-chemical conversion of sewage sludge based on waste heat cascade recovery of copper slag: Mass and energy analysis. *Energy* **2021**, *235*, 121327.
7. Shao, J.; Yan, R.; Chen, H.; Yang, H.; Lee, D. Catalytic effect of metal oxides on pyrolysis of sewage sludge. *Fuel Process. Technol.* **2010**, *91*, 1113–1118.
8. Mu'azu, N.D.; Jarrah, N.; Zubair, M.; Alagha, O. Removal of phenolic compounds from water using sewage sludge-based activated carbon adsorption: A review. *Int. J. Environ. Res. Public Health* **2017**, *14*, 1094.
9. Bora, A.P.; Gupta, D.P.; Durbha, K.S. Sewage sludge to bio-fuel: A review on the sustainable approach of transforming sewage waste to alternative fuel. *Fuel* **2020**, *259*, 116262.
10. Guo, J.; Zheng, L.; Li, Z. Microwave drying behavior, energy consumption, and mathematical modeling of sewage sludge in a novel pilot-scale microwave drying system. *Sci. Total Environ.* **2021**, *777*, 146109.

11. Zhang, H.; Bao, L.; Chen, Y.; Xuan, W.; Yuan, Y. Efficiency improvements of the CO-H<sub>2</sub> mixed gas utilization related to the molten copper slag reducing modification. *Process Saf. Environ. Prot.* **2021**, *146*, 292–299.
12. Zhang, B.; Zhang, T.; Niu, L.P.; Liu, N.; Dou, Z.; Li, Z. Moderate dilution of copper slag by natural gas. *JOM* **2017**, *70*, 47–52.
13. Guo, Z.; Zhu, D.; Pan, J.; Zhang, F. Innovative methodology for comprehensive and harmless utilization of waste copper slag via selective reduction-magnetic separation process. *J. Clean. Prod.* **2018**, *187*, 910–922.
14. Meng, X.; Li, Y.; Wang, H.; Yang, Y.; McLean, A. Effects of Na<sub>2</sub>O additions to copper slag on iron recovery and the generation of ceramics from the non-magnetic residue. *J. Hazard. Mater.* **2020**, *399*, 122845.
15. Gorai, B.; Jana, R.K. Premchand Characteristics and utilisation of copper slag—A review. *Resour. Conserv. Recycl.* **2003**, *39*, 299–313.
16. Gao, C.; Yu, W.; Zhu, Y.; Wang, M.; Tang, Z.; Du, L.; Hu, M.; Fang, L.; Xiao, X. Preparation of porous silicate supported micro-nano zero-valent iron from copper slag and used as persulfate activator for removing organic contaminants. *Sci. Total Environ.* **2021**, *754*, 142131.
17. Li, H.; Zhang, W.; Wang, J.; Yang, Z.; Li, L.; Shih, K. Copper slag as a catalyst for mercury oxidation in coal combustion flue gas. *Waste Manag.* **2018**, *74*, 253–259.
18. Wang, Q.; Li, Z.; Li, D.; Tian, Q.; Guo, X.; Yuan, Z.; Zhao, B.; Wang, Z.; Wang, Y.; Qu, S.; et al. A Method of High-quality Silica Preparation from Copper Smelting Slag. *Jom* **2020**, *72*, 2676–2685.
19. Zuo, Z.; Yu, Q.; Luo, S.; Zhang, J.; Zhou, E. Effects of CaO on two-step reduction characteristics of copper slag using biochar as reducer: Thermodynamic and kinetics. *Energy Fuels* **2020**, *34*, 491–500.
20. Gerasimov, G.; Khaskhachikh, V.; Potapov, O.; Dvoskin, G.; Kornileva, V.; Dudkina, L. Pyrolysis of sewage sludge by solid heat carrier. *Waste Manag.* **2019**, *87*, 218–227.
21. Luo, S.; Fu, J.; Zhou, Y.; Yi, C. The production of hydrogen-rich gas by catalytic pyrolysis of biomass using waste heat from blast-furnace slag. *Renew. Energy* **2017**, *101*, 1030–1036.
22. Li, P. Thermodynamic analysis of waste heat recovery of molten blast furnace slag. *Int. J. Hydrog. Energy* **2017**, *42*, 9688–9695.
23. Zhang, Q.; Liu, H.; Zhang, X.; Lu, G.; Wang, J.; Hu, H.; Li, A.; Yao, H. Effect of Fe/Ca-based composite conditioners on syngas production during different sludge gasification stages: Devolatilization, volatiles homogeneous reforming and heterogeneous catalyzing. *Int. J. Hydrog. Energy* **2017**, *42*, 29150–29158.
24. Widayatno, W.B.; Guan, G.; Rizkiana, J.; Hao, X.; Wang, Z.; Samart, C.; Abudula, A. Steam reforming of tar derived from Fallopia Japonica stem over its own chars prepared at different conditions. *Fuel* **2014**, *132*, 204–210.
25. Huang, Z.; Xu, G.; Deng, Z.; Zhao, K.; He, F.; Chen, D.; Wei, G.; Zheng, A.; Zhao, Z.; Li, H. Investigation on gasification performance of sewage sludge using chemical looping gasification with iron ore oxygen carrier. *Int. J. Hydrog. Energy* **2017**, *42*, 25474–25491.
26. Ma, Z.; Gao, N.; Xie, L.; Li, A. Study of the fast pyrolysis of oilfield sludge with solid heat carrier in a rotary kiln for pyrolytic oil production. *J. Anal. Appl. Pyrolysis* **2014**, *105*, 183–190.
27. Al-Zareer, M.; Dincer, I.; Rosen, M.A. Analysis and assessment of a hydrogen production plant consisting of coal gasification, thermochemical water decomposition and hydrogen compression systems. *Energy Convers. Manag.* **2018**, *157*, 600–618.
28. Zuo, Z.; Luo, S.; Liu, S.; Zhang, J.; Yu, Q.; Bi, X. Thermokinetics of mass-loss behavior on direct reduction of copper slag by waste plastic char. *Chem. Eng. J.* **2021**, *405*, 126671.
29. Feng, Y.; Yang, Q.; Zuo, Z.; Luo, S.; Ren, D.; Lin, H. Study on preparation of oxygen carrier using copper slag as precursor. *Front. Energy Res.* **2021**, *9*, 736. <https://doi.org/10.3389/fenrg.2021.781914>.
30. Sun, Y.; Zhang, Z.; Liu, L.; Wang, X. Two-stage high temperature sludge gasification using the waste heat from hot blast furnace slags. *Bioresour. Technol.* **2015**, *198*, 364–371.
31. Zhao, L.; Wang, H.; Qing, S.; Liu, H. Characteristics of gaseous product from municipal solid waste gasification with hot blast furnace slag. *J. Nat. Gas Chem.* **2010**, *19*, 403–408.
32. Luo, S.; Wang, J.; Guo, X.; Liu, Z.; Sun, W. The production of hydrogen-rich gas by wet sludge gasification using waste heat of blast-furnace slag: Mass and energy balance analysis. *Int. J. Hydrog. Energy* **2019**, *44*, 5171–5175.
33. Deng, S.; Hu, J.; Wang, H.; Li, J.; Hu, W. Catalytic gasification of pre-calcined copper slag and biomass mixture. *Chin. J. Environ. Eng.* **2013**, *7*, 3148–3152.
34. Zhao, L.; Hu, J.; Wang, H.; Liu, H.; Qing, S.; Li, L. Influence of Pre-calcined Copper-containing Slag on Catalytic Pyrolysis Kinetics of Biomass. *Chin. J. Process Eng.* **2010**, *10*, 726–731.